

## Two-Center/Three-Electron Sigma Half-Bonds in Main Group and Transition Metal Chemistry

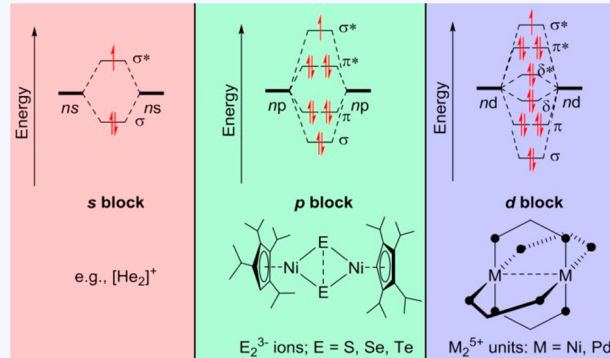
John F. Berry\*

Department of Chemistry, University of Wisconsin—Madison, 1101 University Avenue, Madison, Wisconsin 53706, United States

**CONSPECTUS:** First proposed in a classic Linus Pauling paper, the two-center/three-electron ( $2c/3e$ )  $\sigma$  half-bond challenges the extremes of what may or may not be considered a chemical bond. Two electrons occupying a  $\sigma$  bonding orbital and one electron occupying the antibonding  $\sigma^*$  orbital results in bond orders of  $\sim 0.5$  that are characteristic of metastable and exotic species, epitomized in the fleetingly stable  $\text{He}_2^+$  ion.

In this Account, I describe the use of coordination chemistry to stabilize such fugacious three-electron bonded species at disparate ends of the periodic table. A recent emphasis in the chemistry of metal–metal bonds has been to prepare compounds with extremely short metal–metal distances and high metal–metal bond orders. But similar chemistry can be used to explore metal–metal bond orders less than one, including  $2c/3e$  half-bonds. Bimetallic compounds in the  $\text{Ni}_{2(\text{II,III})}$  and  $\text{Pd}_{2(\text{II,III})}$  oxidation states were originally examined in the 1980s, but the evidence collected at that time suggested that they did not contain  $2c/3e$   $\sigma$  bonds. Both classes of compounds have been re-examined using EPR spectroscopy and modern computational methods that show the unpaired electron of each compound to occupy a  $\text{M–M } \sigma^*$  orbital, consistent with  $2c/3e$   $\text{Ni–Ni}$  and  $\text{Pd–Pd } \sigma$  half-bonds.

Elsewhere on the periodic table, a seemingly unrelated compound containing a trigonal bipyramidal  $\text{Cu}_3\text{S}_2$  core caused a stir, leaving prominent theorists at odds with one another as to whether the compound contains a  $\text{S–S}$  bond. Due to my previous experience with  $2c/3e$  metal–metal bonds, I suggested that the  $\text{Cu}_3\text{S}_2$  compound could contain a  $2c/3e$   $\text{S–S } \sigma$  half-bond in the previously unknown oxidation state of  $\text{S}_2^{3-}$ . By use of the Cambridge Database, a number of other known compounds were identified as potentially containing  $\text{S}_2^{3-}$  ligands, including a noteworthy set of cyclopentadienyl-supported compounds possessing diamond-shaped  $\text{Ni}_2\text{E}_2$  units with  $\text{E} = \text{S, Se, Te}$ . These compounds were subjected to extensive studies using X-ray absorption spectroscopy, X-ray photoelectron spectroscopy, density functional theory, and wave function-based computational methods, as well as chemical oxidation and reduction. The compounds contain  $\text{E–E } 2c/3e \sigma$  half-bonds and unprecedented  $\text{E}_2^{3-}$  “subchalcogenide” ligands, ushering in a new oxidation state paradigm for transition metal–chalcogen chemistry.



### INTRODUCTION

In 1931, Pauling introduced the three-electron bond to explain the stability of the paramagnetic gases  $\text{NO}$ ,  $\text{NO}_2$ , and  $\text{O}_2$ .<sup>1,2</sup>

*The approximate solution of the wave equation for a system composed of a pair of electrons attached to one nucleus and a single electron attached to another nucleus has shown that the resonance forces corresponding to interchange of the three electrons are in the main repulsive. Thus, normal He and H have no tendency whatever to molecule formation. But if the two nuclei are identical or nearly so, an additional degeneracy is introduced, for the two configurations A: ·B and A: ·B, in one of which atom A contains an electron pair and B an unpaired electron, and in the other A contains an unpaired electron and B an electron pair, they have nearly the same energy. The interactions of the two atoms will then cause the eigenfunction for the normal state of the system to be the stable nuclear-symmetric combination of the eigenfunctions corresponding to the two configurations; and the accompanying resonance energy will lead to the formation of a stable molecule containing a three-electron bond.*<sup>1</sup>

The quintessential example is the  $\text{He}_2^+$  ion, with the molecular orbital picture given in Chart 1A. Here, the 1s orbitals of each He atom overlap to form a  $\sigma$  bonding and  $\sigma^*$  antibonding combination. The filled  $\sigma$  and half-filled  $\sigma^*$  orbitals result in a net bonding interaction between the two He nuclei, the two-center/three-electron ( $2c/3e$ ) half-bond, denoted here by the symbol  $\text{..}$ . This elementary analysis implies a  $\text{He..He}$  bond order of 0.5, as in the  $\text{H}_2^+$  ion. Unlike  $\text{H}_2^+$ , however, additional repulsive components to the energy arise from the presence of three electrons. Thus,  $2c/3e$   $\sigma$  half-bonds are weak interactions with bond orders from quantum chemical calculations that are  $\leq 0.5$ .<sup>3,4</sup> The alkaline earth metal dimer cations<sup>5,6</sup> and group 12 dimer cations<sup>7,8</sup> share similar  $2c/3e$  bonds formed via s orbital overlap.

The concept of the  $2c/3e$  bond may be readily extended to element dimers,  $\text{E}_2$ , in the p or d block. For p block elements, this requires 15 valence electrons to fill the octet of one atom and 7/8ths of the other atom (Chart 1B). Here, the p orbitals form

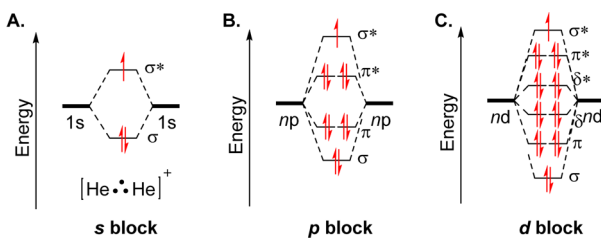
Received: November 20, 2015

Published: January 7, 2016

bonding and antibonding pairs of  $\sigma$  and  $\pi$  symmetry. The bonding  $\sigma$  and two  $\pi$  orbitals are filled along with the two  $\pi^*$  orbitals leaving one electron in the  $\sigma^*$  level. Thus, there remains no net  $\pi$  bonding, and only the partial (three-electron)  $\sigma$  interaction, identical to that in  $\text{He}_2^+$ . The monocationic noble gas (G) dimers of the type  $\text{G}_2^+$  fulfill this valence electron requirement, and one of these, the  $\text{Xe}_2^+$  ion, is stable enough to have been crystallographically characterized with a remarkably long  $\text{Xe}\cdots\text{Xe}$  bond length of  $3.09\text{ \AA}$ .<sup>9</sup> Isoelectronic  $2c/3e$ -bonded species with other p block elements are represented by dihalogen anions,  $\text{X}_2^-$  species, studied by pulse radiolysis.<sup>10</sup> Considering the chalcogen (Ch) elements, a 15-electron  $2c/3e$  half-bond requires a  $\text{Ch}_2^{3-}$  ion, which has never been previously observed.

For transition metals, d orbital overlap forms bonding and antibonding orbital combinations of  $\sigma$ ,  $\pi$ , and  $\delta$  symmetry, and a ( $d^{10}-d^9$ )  $\text{M}\cdots\text{M}$  combination would be required for a  $2c/3e$   $\sigma$  half-bond (Chart 1C). In this case, all  $\sigma$ ,  $\pi$ ,  $\delta$ ,  $\delta^*$ , and  $\pi^*$  orbitals

**Chart 1. Molecular Orbital Schemes for  $2c/3e$  Bonds Formed by Overlap of Two s Orbitals, as in the  $\text{He}_2^+$  Ion (A), the p Orbital Manifold (B), and the d Orbital Manifold (C)**



will be filled with the  $\sigma^*$  orbital half-filled. The only element with a  $nd^{10}(n+1)s^0$  electron configuration that might fulfill this electronic requirement is Pd. To my knowledge, the (presumably  $2c/3e$ -bonded)  $\text{Pd}_2^+$  ion has never been investigated.

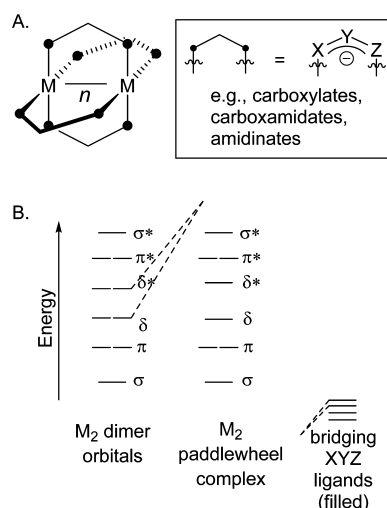
Unsupported E·E  $2c/3e$   $\sigma$  bonds are thus exceedingly rare, with  $\text{Xe}_2^+$  being the only crystallographically characterized example. Coordination chemistry has long been known as a fruitful avenue for stabilizing the unstable. Here, I recount my journey in using coordination chemistry to investigate  $2c/3e$  bonds with both main group and transition elements. The transition element chemistry happened first, chronologically, so that is where this story begins.

## ■ 2c/3e BONDS IN TRANSITION METAL CHEMISTRY

The tetragonal paddlewheel motif shown in Chart 2 has been the focus of numerous studies on metal–metal bonds.<sup>11</sup> The four equatorial ligands raise the energy of one set of  $\text{M}_2/\delta/\delta^*$  orbitals (the ones directed along the bonds to the equatorial ligands) such that they can essentially be excluded from the MO diagram. Due to this modification, the number of electrons needed to yield a  $\text{M}\cdots\text{M}$   $2c/3e$  bond in tetragonal symmetry is 15, or a combination of ( $d^8-d^7$ ) metal ions. This can be achieved either by reduction of a ( $d^7-d^7$ ) dimer or by oxidation of a ( $d^8-d^8$ ) dimer. The latter possibility is discussed here.

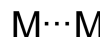
Though significant work on  $\text{Rh}_2$ ,  $\text{Ir}_2$ , and  $\text{Au}_2$  compounds has been reported,<sup>12</sup> the most common ( $d^8-d^8$ ) dimers involve the group 10 metals Ni, Pd, and Pt. The 16 valence electrons of these metal centers fill the MO diagram of Chart 2B, leading to the conclusion that these compounds have no metal–metal bond, by virtue of having all bonding and antibonding orbitals filled. This zeroth order analysis is largely correct, but there is more nuance to the electronic structure.<sup>13</sup> Due to the proximity

**Chart 2. (A) Tetragonal Paddlewheel Structure and (B) d Orbital Manifold for Tetragonal Paddlewheel Complexes**



of the two metals, the  $\text{M}_2 \sigma^*$  orbital is raised high enough in energy that it is able to mix with the  $(n+1)s$  and even the  $(n+1)p$  orbitals. Hybridization of the  $\sigma^*$  orbital has the effect shown in Chart 3, resulting in an orbital that is more nonbonding in

**Chart 3. Effect of d/s/p Hybridization of a  $\text{M}\cdots\text{M} \sigma^*$  Orbital**



character than antibonding. The lower-energy  $\text{M}_2 \sigma$  orbital does not undergo this hybridization effect. Thus, the  $\text{M}_2 \sigma$  orbital has stronger bonding character than the  $\text{M}_2 \sigma^*$  orbital has antibonding character, and the  $d^8-d^8$  dimers therefore have residual  $\text{M}\cdots\text{M} \sigma$  bonding with small but nonzero bond orders calculated from DFT.<sup>13</sup>

Nonetheless, removal of an electron from the  $\text{M}_2 \sigma^*$  orbital should produce a three-electron  $\text{M}\cdots\text{M} \sigma$  half-bond. Single occupation of a  $\text{M}_2 \sigma^*$  orbital should have an effect on the order of  $0.5\text{ \AA}$  on the  $\text{M}\cdots\text{M}$  separation,<sup>14</sup> as observed for the first  $2c/3e$  metal–metal half-bond in an organometallic compound.<sup>15</sup> Due to the nonbonding character of the  $\sigma^*$  orbital, however, the actual changes in  $\text{M}\cdots\text{M}$  separations here will be significantly less than this estimate.

Oxidation of  $d^8-d^8$  dimers of Ni(II) and Pd(II) was first investigated in 1988 in the paper F. A. Cotton celebrated as his 1000th publication.<sup>16</sup> Similar Pt chemistry was reported later.<sup>17</sup> In these studies,  $\text{M}_2(\text{II},\text{II})$  complexes supported by bridging, bidentate  $N,N'$ -bis(4-methylphenyl)formamidinate ((*p*-methyl)form) ligands ( $X = Z = \text{N}-\text{Ar}$ ,  $Y = \text{CH}$  in Chart 2A) were oxidized to their corresponding  $[\text{M}_2((p\text{-methyl})\text{form})_4]^+$  monocations. In terms of the search for  $2c/3e$   $\sigma$ -bonded species, the results of structural analyses, EPR spectroscopy, and computational (SCF-X $\alpha$ -SW) studies were somewhat disappointing. Oxidation of  $\text{Ni}_2((p\text{-methyl})\text{form})_4$  to  $[\text{Ni}_2((p\text{-methyl})\text{form})_4]^+$  resulted in a contraction of the Ni–Ni distance by a modest  $0.07\text{ \AA}$  (Table 1), and an EPR spectrum of the cation suggested a

**Table 1. Comparison of Metal–Metal Bond Lengths<sup>a</sup> in  $(\text{Ni}_2)^{4+/5+}$  and  $(\text{Pd}_2)^{4+/5+}$  Dimers**

compound	Ni <sub>2</sub> Compounds			$\Delta d_{\text{Ni–Ni}}$ (Å)	ref
	Ni(II)–Ni(II) (Å)	Ni(II)–Ni(III) (Å)	$\Delta d_{\text{Ni–Ni}}$ (Å)		
$\text{Ni}_2((p\text{-methyl form})_4$	2.487[3]	2.418(4)	0.069(4)	16	
$\text{Ni}_2((p\text{-methoxy form})_4$	2.476(1)	2.3703(4)	0.106(1)	18	
$\text{Ni}_2(\text{tpg})_4$	2.4280(5)	2.3298(6)	0.0982(6)	18	
compound	Pd <sub>2</sub> Compounds			$\Delta d_{\text{Pd–Pd}}$ (Å)	ref
	Pd(II)–Pd(II) (Å)	Pd(II)–Pd(III) (Å)	$\Delta d_{\text{Pd–Pd}}$ (Å)		
$\text{Pd}_2((p\text{-methyl form})_4$	2.622(3)	2.637(6)	-0.015(6)	16	
$\text{Pd}_2((p\text{-methoxy form})_4$	2.6486(8)	2.597(1)	0.053(1)	21	

<sup>a</sup> Parentheses indicate esds for single crystallographic measurements whereas brackets are used for averaged values.

Ni-centered unpaired electron. Calculations suggested, however, that the SOMO was the  $\text{Ni}_2 \delta^*$  orbital rather than the expected  $\sigma^*$  orbital. In the case of the Pd<sub>2</sub> dimers, oxidation caused an *increase* in the Pd–Pd distance by 0.015 Å; the EPR and computational data suggested that an amidinate ligand, rather than the Pd<sub>2</sub> center, had been oxidized.<sup>16</sup>

My co-workers and I reinvestigated this Ni<sub>2</sub> and Pd<sub>2</sub> chemistry in work that spanned my time between graduate studies at Texas A&M University, postdoctoral work at the Max Planck Institute for Bioinorganic Chemistry (now Chemical Energy Conversion), and work as an Assistant Professor at the University of Wisconsin—Madison.

### Ni<sup>·</sup>·Ni Three-Electron Bonds

One example does not make a trend. To reinvestigate Ni<sub>2</sub>(II,III) chemistry, we began by synthesizing new Ni<sub>2</sub>(II,III) compounds. In addition to the (*p*-methyl)form ligand used in the 1988 study, we prepared the corresponding (*p*-methoxy)form and triphenylguanidinate (tpg; X = Z = NPh; Y = CN(H)Ph) Ni<sub>2</sub>(II,II) complexes and oxidized them to the Ni<sub>2</sub>(II,III) level.<sup>18</sup> Both of these ligands are more electron rich than the (*p*-methyl)form ligand, which resulted in significantly lower Ni<sub>2</sub><sup>4+/5+</sup> redox potentials and more thermally stable Ni<sub>2</sub>(II,III) complexes. Crystal structures for these compounds were determined in both the Ni<sub>2</sub>(II,II) and Ni<sub>2</sub>(II,III) oxidation states (Figure 1). We were

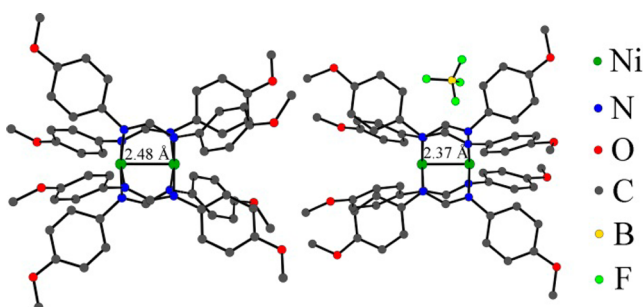


**Figure 1.** Molecular structures of  $\text{Ni}_2((p\text{-methoxy})\text{form})_4$  and  $[\text{Ni}_2((p\text{-methoxy})\text{form})_4]\text{BF}_4$ , with hydrogen atoms removed for clarity.

surprised to find that, in the complexes of the more electron rich ligands, the shortening of the Ni–Ni distances ( $\Delta d_{\text{Ni–Ni}}$ , defined as the (Ni<sub>2</sub>)<sup>4+</sup> distance minus the (Ni<sub>2</sub>)<sup>5+</sup> distance) was significantly more than it had been in the (*p*-methyl)form compound,

on the order of ~0.1 Å (see Table 1). In fact, this  $\Delta d_{\text{Ni–Ni}}$  value falls outside the range of expected changes upon population/ depopulation of  $\delta$  orbitals (0.03–0.07 Å).<sup>11,14</sup> This was our first hint that the supposed  $(\delta^*)^1$  ground state for (Ni<sub>2</sub>)<sup>5+</sup> compounds could be incorrect.

The next hint came from an EPR study of the new Ni<sub>2</sub>(II,III) compounds. At room temperature, an isotropic EPR signal at  $g = 2.16$  is observed for  $[\text{Ni}_2(\text{tpg})_4]^+$ , which is consistent with the 1988 results and indicates a Ni<sub>2</sub>-centered unpaired electron. For  $[\text{Ni}_2((p\text{-methoxy})\text{form})_4]^+$ , a low temperature EPR spectrum in frozen acetonitrile displayed an axial signal ( $g_{\perp} = 2.234$ ,  $g_{\parallel} = 2.045$ ) with the  $g_{\parallel}$  component split into a 1:1:1 triplet, indicating hyperfine coupling to an  $I = 1$  <sup>14</sup>N nucleus. The  $[\text{Ni}_2((p\text{-methoxy})\text{form})_4]^+$  ion was thus proposed to bind a single solvent molecule along the Ni–Ni axis, giving rise to coupling of a  $\sigma^*$  unpaired electron with the N atom of the acetonitrile.

In 1988, the strongest piece of evidence for a Ni<sub>2</sub>  $(\delta^*)^1$  ground state came from computations,<sup>16</sup> but the methods used are antiquated by today's standards. So the electronic structure was reinvestigated using modern DFT methods. Like in the 1988 study, we first examined a truncated model of the Ni<sub>2</sub>(II,II) compounds that used [HNC(H)NH]<sup>-</sup> ligands, in idealized  $D_{4h}$  symmetry. This model revealed two important frontier orbitals, the Ni<sub>2</sub>  $\sigma^*$  orbital of  $a_{2u}$  symmetry and a ligand  $\pi(\text{nb})$  orbital of  $a_{1u}$  symmetry (Figure 2). In the Ni<sub>2</sub>(II,II) state, both of these

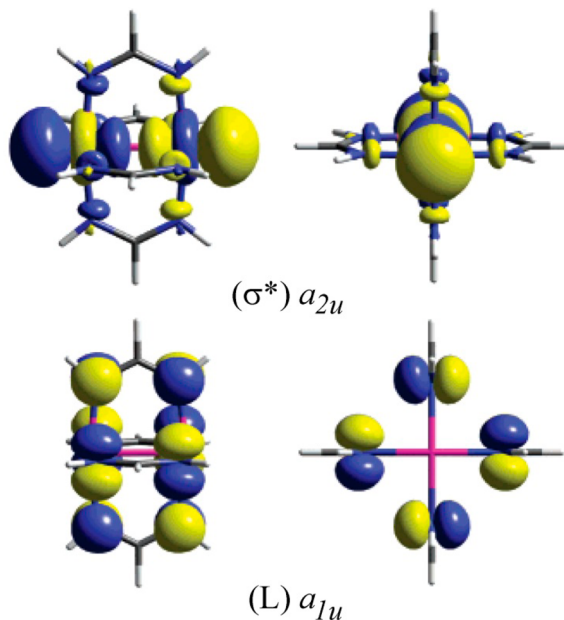


**Figure 2.** Important orbitals of the  $\text{Ni}_2(\text{HNC(H)NH})_4$  molecule. Adapted from ref 18. Copyright 2006 American Chemical Society.

orbitals are occupied, so their ordering determines the nature of the oxidized Ni<sub>2</sub>(II,III) complex, under the assumption of Koopmans' theorem. Consistent with the redox behavior of these compounds, the equatorial ligand plays an important role in the electronic structure. With the simple Ni<sub>2</sub>(HNC(H)NH)<sub>4</sub> model compound, the ligand-centered  $a_{1u}$  orbital was predicted to be highest in energy, but upon performing a calculation including the entire Ni<sub>2</sub>((*p*-methoxy)form)<sub>4</sub> molecule, the ordering between the  $a_{1u}$  and  $a_{2u}$  orbitals became reversed, and even without taking into account the binding of an axial ligand, these results therefore predicted that the Ni<sub>2</sub>(II,III) species would have a  $(\sigma^*)^1$  ground state with a Ni<sup>·</sup>·Ni three-electron  $\sigma$  half-bond.<sup>18</sup>

### Pd<sub>2</sub>:Pd Three-Electron Bonds

Reinvestigation of the  $[\text{Pd}_2(\text{form})_4]^+$  case required a slightly different approach. The 1988 computational data indicated a ligand-centered unpaired electron, and the isotropic EPR signal with  $g = 2.014$  was strong supporting evidence.<sup>16</sup> Moreover, an elongation of the Pd–Pd distance upon oxidation was inconsistent with any Pd<sub>2</sub>-centered redox model.<sup>16</sup> However, two important developments caused us to question this interpretation. The first was a report from Bear and co-workers of the  $\text{Pd}_2(\text{benz})_4$  compound (benz = *N,N*-diphenylbenzimidinate; X = Z = NPh, Y = CPh).<sup>19</sup>  $\text{Pd}_2(\text{benz})_4$  was oxidized electrochemically by one electron, and the EPR spectrum of the resulting species was sharp and axial with clear <sup>105</sup>Pd hyperfine coupling consistent with a Pd<sub>2</sub>-centered redox process.<sup>19</sup> However, no crystal structure of the  $[\text{Pd}_2(\text{benz})_4]^+$  cation was reported, so it was not possible to say with certainty whether the electrochemically generated EPR active species retained the Pd<sub>2</sub> paddlewheel-type structure. The second development was the discovery of the first Pd<sub>2</sub>(III,III) paddlewheel-type dimer,  $\text{Pd}_2(\text{hpp})_4\text{Cl}_2$  (hpp = 1,3,4,6,7,8-hexahydro-2*H*-pyrimido[1,2-*a*]pyrimidinate), for which computations indicated a full Pd–Pd  $\sigma$  bond.<sup>20</sup>

Thus, we set out to reinvestigate  $[\text{Pd}_2((p\text{-methyl})\text{form})_4]^+$  and also its more stable  $[\text{Pd}_2((p\text{-methoxy})\text{form})_4]^+$  analog.<sup>21</sup> As in the case of the Ni<sub>2</sub> compounds,  $\Delta d_{\text{Pd–Pd}}$  became larger with more electron-rich ligands. Thus,  $[\text{Pd}_2((p\text{-methoxy})\text{form})_4]^+$  has a Pd–Pd distance that is 0.05 Å shorter than its Pd<sub>2</sub>(II,II) precursor, consistent with Pd<sub>2</sub>-centered oxidation. However, the EPR spectrum of the  $[\text{Pd}_2((p\text{-methoxy})\text{form})_4]^+$ , shown in Figure 3A, is

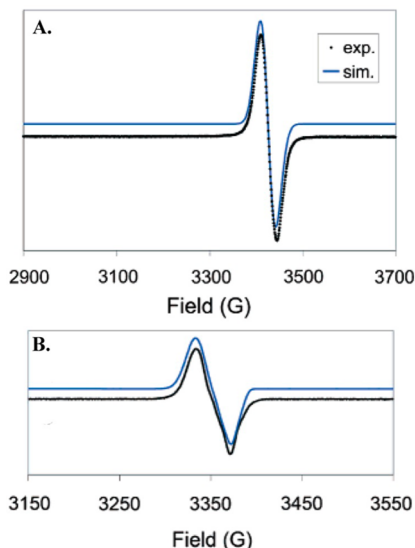


**Figure 3.** X-band EPR spectra of  $[\text{Pd}_2((p\text{-methoxy})\text{form})_4]^+$  in (A) frozen  $\text{CH}_2\text{Cl}_2$  solution and (B) frozen butyronitrile solution. Adapted from ref 21. Copyright 2007 American Chemical Society.

nearly identical to that of its  $[\text{Pd}_2((p\text{-methyl})\text{form})_4]^+$  analog: broad and isotropic with a  $g$  value of 2.01. Since we learned from the Ni<sub>2</sub> chemistry that nitrile binding can affect the EPR spectrum, we decided to investigate the EPR spectrum of  $[\text{Pd}_2((p\text{-methoxy})\text{form})_4]^+$  in frozen butyronitrile solution. The resulting spectrum, shown in Figure 3B, is still broad and nearly isotropic, but there are clear shoulder features that indicate hyperfine structure. The spectrum was modeled with a coupling to two symmetry-equivalent axial <sup>14</sup>N nuclei derived from butyronitrile. This model strongly suggests a  $(\sigma^*)^1$  ground state.

For further support of this assignment, we brought out the big guns: high-field EPR measurements of both  $[\text{Pd}_2((p\text{-methyl})\text{form})_4]^+$  and  $[\text{Pd}_2((p\text{-methoxy})\text{form})_4]^+$  were made from Q-band (34 GHz) to D band at ~210 GHz.<sup>21</sup> At these high frequencies the EPR spectra were much better resolved, and the true  $g$  anisotropy became apparent. At 210 GHz,  $[\text{Pd}_2((p\text{-methyl})\text{form})_4]^+$  was found to show an axial spectrum with  $g_{\perp} = 2.03$  and  $g_{\parallel} = 1.99$ , whereas  $[\text{Pd}_2((p\text{-methoxy})\text{form})_4]^+$  was rhombic with  $g_1 = 2.03$ ,  $g_2 = 2.01$ , and  $g_3 = 2.00$ . The anisotropies in these spectra clearly indicate Pd<sub>2</sub>-centered oxidation and are not consistent with ligand-based oxidation.

For the Pd<sub>2</sub> compounds, DFT calculations on the truncated models  $\text{Pd}_2(\text{HNC(H)NH})_4$  and  $[\text{Pd}_2(\text{HNC(H)NH})_4]^+$  directly predict a  $(\sigma^*)^1$  ground state for the Pd<sub>2</sub>(II,III) species, and not ligand oxidation.<sup>21</sup> Thus, after 20 years of ambiguity, these compounds with M:M 2c/3e  $\sigma$  half-bonds are now well-described.

### ■ 2c/3e BONDS IN MAIN GROUP CHEMISTRY

With this transition metal chemistry as a prelude, I then stumbled into the topic of 2c/3e bonds in main group chemistry by sheer happenstance. In 2009, I read a paper by Alvarez, Hoffmann, and Mealli (abbreviated here as AHM) with an intriguing title: “A Bonding Quandary—or—A Demonstration of the Fact That Scientists Are Not Born With Logic”.<sup>22</sup> The topic of this paper was the compound shown in Figure 4, a triangular Cu<sub>3</sub> complex

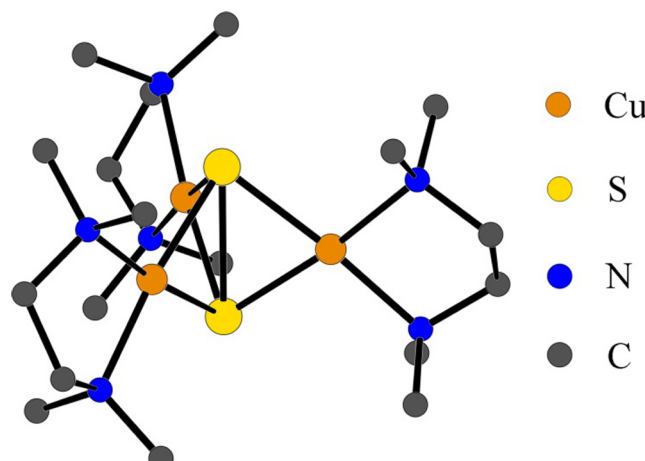
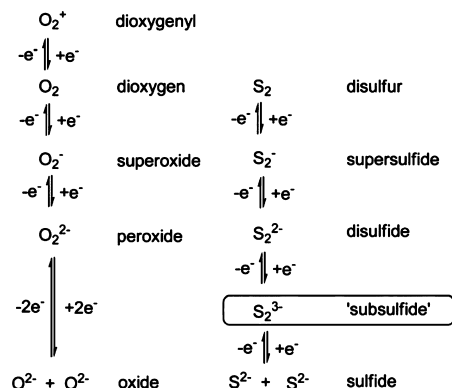


**Figure 4.** Molecular structure of the  $[\text{Cu}_3\text{S}_2(\text{tmada})_3]^{3+}$  trication; hydrogen atoms and counteranions are not shown.

with two capping S atoms that had been reported by Tolman and co-workers in 2005.<sup>23</sup> The “bonding quandary” was the question of whether the compound contains a S–S bond, that is, whether the compound contains two nonbonded  $\text{S}^{2-}$  ligands or a singly bonded  $\text{S}_2^{2-}$  ligand. The three authors could not agree with each other on this topic and in fact provided strong arguments against both the  $(2 \times \text{S}^{2-})$  and  $\text{S}_2^{2-}$  assignments.<sup>22</sup> I had not even finished reading the (lengthy, but entertaining!) paper before asking myself “Why do AHM not consider an  $\text{S}_2^{3-}$  ligand?” So, I began to consider it.

The extensive redox chemistry of  $\text{O}_2$  (Scheme 1, left) is of critical importance to all life on Earth. The two-electron peroxide/oxide redox couple is particularly significant in that it involves making and breaking an O–O bond, key processes in the function of photosynthesis and respiration.<sup>24</sup> Redox chemistry of  $\text{S}_2$  (Scheme 1, right) was previously assumed to be analogous to that of  $\text{O}_2$ , with the distinction that  $\text{S}_2$  itself is not

**Scheme 1. Comparison of the Redox Chemistry of O<sub>2</sub> and S<sub>2</sub>**



the most stable allotrope of sulfur. The idea of an  $S_2^{3-}$  species implies a 2c/3e S:S half-bond and, formally, a previously unknown oxidation state for elemental sulfur. In its uncombined form, sulfur is only known to form three paramagnetic species: free  $^3P$  atomic S; diatomic  $S_2$ , isoelectronic to  $O_2$ ; and  $S_2^-$ , isoelectronic to the superoxide ion.<sup>25</sup> In analogy to the name “supersulfide” for  $S_2^-$ , I decided to call the  $S_2^{3-}$  ion “sub sulfide.”<sup>26</sup>

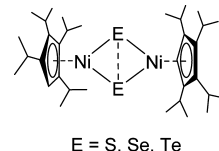
Although the parent  $S_2^{3-}$  ion is unknown, precedents exist for three-electron  $\sigma$ -bonded species in unstable organic  $[RCh\cdot:ChR]^-$  radical anions,<sup>27</sup> as well as  $[R_2Ch\cdot:ChR_2]^+$  radical cations,<sup>28</sup> and other related unstable species.<sup>29</sup> Structural features of these species have been calculated,<sup>30</sup> and recently a crystal structure of a radical cation species has been reported.<sup>28</sup> Noteworthy is the observed shortening of the nonbonding S··S distance from 3.02 to 2.82 Å in the radical cation,<sup>28</sup> consistent with the removal of an electron from the S–S  $\sigma^*$  orbital.

Could Tolman's  $\text{Cu}_3\text{S}_2$  compound contain three-electron-bonded  $\text{S}_2^{3-}$  as a ligand? Consider the available experimental data: (1) The three Cu atoms are crystallographically equivalent in the solid state and magnetically equivalent in solution. Either a  $(2 \times \text{S}^{2-})$  or an  $\text{S}_2^{2-}$  model would require Cu mixed-valency in which the three Cu ions would most likely be inequivalent. (2) The S···S distance of 2.73 Å falls directly between the distances in crystallographically characterized  $\text{M}_2\text{S}_2$  and  $\text{M}_3\text{S}_2$  compounds that correspond to singly bonded  $\text{S}_2^{2-}$  ligands (~2.00 Å) and nonbonded  $\text{S}^{2-}$  ligands (~3.30 Å). (3) The observed spin triplet ground state of **1** is consistent with antiferromagnetic coupling of an  $\text{S}_2$  radical with each of the three  $\text{S} = 1/2 \text{ Cu}^{2+}$  ions. Based on these considerations and supporting computations, I then published a suggestion that this compound could contain an  $\text{S}_2^{3-}$  subsulfido ligand.<sup>26</sup> The above data are consistent with the existence of the subsulfide ion in **1**, but as I pointed out,<sup>26</sup> they are not unambiguously definitive.

With the suggestion that the  $S_2^{3-}$  ion could serve as a ligand to transition metals, it seemed to me most prudent to find new examples of compounds that might behave similarly. My first instinct was that other subsulfido compounds probably exist and perhaps were already known but were not recognized as being  $S_2^{3-}$  compounds. A search of the Cambridge Structural Database for  $S_2$ -containing transition metal compounds with S-S distances between 2.00 and 3.30 Å provided a number of hits. My attention was immediately drawn to a fascinating set of compounds containing a  $Ni_2E_2$  diamond core reported in 2001 by Sitzmann and co-workers (Chart 4),<sup>31</sup> with  $S_2$ ,  $Se_2$ , and  $Te_2$  ligands.

Sitzmann and co-workers recognized the unusual E···E interactions in these  $\text{Cp}'_2\text{Ni}_2\text{E}_2$  compounds from their electrochemical

**Chart 4. Molecular Structure of  $Cp'_2Ni_2E_2$  Compounds**



investigation of the series, stating “The complexes...appear to be neither Ni(II) complexes with an  $E_2^{2-}$  bridge nor Ni(III) complexes with two  $E^{2-}$  bridges.”<sup>31</sup> However, an  $E_2^{3-}$  electronic configuration was not proposed. In order to further assess the nature of the E···E bonding in these compounds, we opened three lines of inquiry: spectroscopic investigation of the  $Cp'_2Ni_2E_2$  compounds, computational assessment of their electronic structure, and chemical oxidation and reduction of the compounds. Concurrent with our investigations, Driess and co-workers developed synthetic methods deliberately targeting the preparation of new  $S_2^{3-}$  compounds.<sup>32,33</sup>

## Spectroscopy

X-ray absorption spectroscopy (XAS) is widely used to assess oxidation states in coordination compounds and has been successful at resolving electronic structural problems in complexes containing redox-active sulfur-containing ligands.<sup>34</sup> In principle, S K-edge XAS can be used to probe the relative oxidation level of S<sub>2</sub> and occupancy of the S–S  $\sigma^*$  orbital. The energy of the S rising edge, corresponding to a fully allowed S 1s  $\rightarrow$  4p transition, can be correlated to S oxidation states, while the 1s  $\rightarrow$   $\sigma^*$  transition occurs as a prominent pre-edge transition. In practice, the S K-edge XAS data for Cp'<sub>2</sub>Ni<sub>2</sub>S<sub>2</sub> are not as easy to interpret. Due to the strong covalency of the Ni–S bonds, there are several unoccupied orbitals in the compound that have Ni–S antibonding character (vide infra), all of which contribute to a strong pre-edge feature in the S XAS spectrum.<sup>35</sup> Because of the prominence of this pre-edge transition, accurate edge energies are difficult to determine. Thus, while S XAS of Cp'<sub>2</sub>Ni<sub>2</sub>S<sub>2</sub> does indicate the presence of empty orbitals with S character, a detailed interpretation requires comparison to a computational model.

The situation improves dramatically when the Se K-edge XAS data of  $\text{Cp}'_2\text{Ni}_2\text{Se}_2$  are considered. Here, the Se rising edge is so broad that any pre-edge transitions are within the envelope of the main line. Thus, only the energy of the rising edge can be accurately determined. Although this results in a loss of information about the valence orbitals, it allows us to compare directly Se K-edge energies for a set of compounds with known Se oxidation states ranging from +6 in  $\text{SeO}_4^{2-}$  to -1 in  $\text{Na}_2\text{Se}_2$  (Figure 5). These follow the expected trend, with a decrease in the edge energy as the Se oxidation number decreases. The Sitzmann  $\text{Cp}'_2\text{Ni}_2\text{Se}_2$  compound has an edge energy lower than all of the compounds in our test set, which, via extrapolation of the linear trend in Se oxidation states, corresponds to an oxidation state of -1.5 for the Se atoms in the compound, indicative of an  $\text{Se}_2^{3-}$  ligand.<sup>36</sup>

In a similar fashion, X-ray photoelectron spectroscopy (XPS) data correlate with the Ni oxidation states of the Sitzmann compounds. These experiments probe the binding energies of the Ni 2p core electrons. We compared the  $2p_{3/2}$  energies of  $\text{Cp}'_2\text{Ni}_2\text{S}_2$  and  $\text{Cp}'_2\text{Ni}_2\text{Se}_2$  with known compounds in the Ni(II) and Ni(III) oxidation states also supported by the  $\text{Cp}'$  ligand, and found (Figure 6) that the XPS signals for the chalcogen compounds fall between these Ni(II) and Ni(III) references,

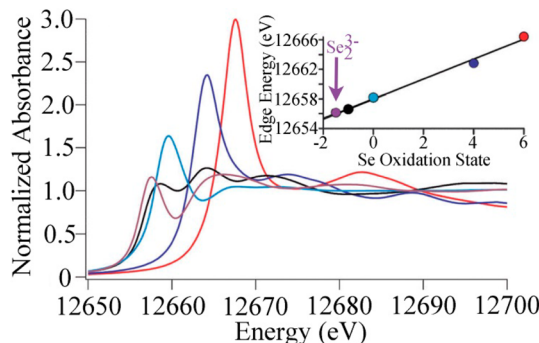


**Figure 5.** Se K edge X-ray absorption spectra of  $\text{Na}_2\text{SeO}_4$  (red),  $\text{Na}_2\text{SeO}_3$  (dark blue), elemental Se (light blue),  $\text{Na}_2\text{Se}_2$  (black), and  $\text{Cp}'_2\text{Ni}_2\text{Se}_2$  (purple). Inset: Correlation of the Se edge energies with Se oxidation states, including the data point for  $\text{Cp}'_2\text{Ni}_2\text{Se}_2$  suggesting a Se oxidation state of  $-1.5$ . Figure adapted from ref 36. Copyright 2012 John Wiley and Sons.

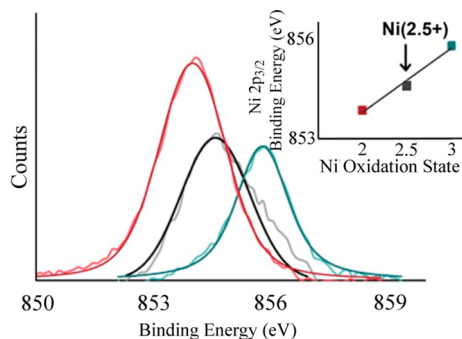


**Figure 6.** Ni  $2p_{3/2}$  region of the X-ray photoelectron spectra of  $[\text{Cp}'_2\text{Ni}] \text{BF}_4$  (blue),  $\text{Cp}'_2\text{Ni}_2\text{S}_2$  (black), and  $[\text{Cp}_2\text{Co}][\text{Cp}'_2\text{Ni}_2\text{S}_2]$  (red). Inset: Correlation of the Ni  $2p_{3/2}$  energies with Ni oxidation state. Figure adapted from ref 35. Copyright 2015 American Chemical Society.

suggesting a delocalized, mixed valent  $\text{Ni}_2(\text{II,III})$  core in the  $\text{Cp}'_2\text{Ni}_2\text{E}_2$  compounds. The  $\text{Ni}_2(\text{II,III})$  oxidation states are wholly consistent with an  $\text{E}_2^{3-}$  oxidation state for the dichalcogen unit. The similarities of the spectroscopic features for these three compounds mean that they can be established spectroscopically to contain  $2c/3e$ -bonded  $\text{S}_2^{3-}$ ,  $\text{Se}_2^{3-}$ , and  $\text{Te}_2^{3-}$  ligands.<sup>35</sup>

### Computations

A three-electron bonded  $[\text{S}:\text{S}]^{3-}$  species should have an unpaired electron, but  $\text{Cp}'_2\text{Ni}_2\text{S}_2$  is diamagnetic. A molecular orbital analysis of the compound was therefore made, taking into account all the possible orbital interactions between the  $\text{S}_2$  unit and the  $\text{Cp}'\text{Ni}$  fragments. The essential details are given in Figure 7, highlighting the frontier orbital region. The key feature here is the  $\text{S}-\text{S} 2c/3e$  interaction, which leaves a singly occupied  $\text{S}-\text{S} \sigma^*$  orbital close in energy to a singly occupied  $\text{Ni}_2$  orbital combination of the appropriate symmetry for these  $\text{S}_2$  and  $\text{Ni}_2$  orbitals to mix strongly. Thus, the bonding  $\text{Ni}_2\text{S}_2$  combination becomes doubly occupied while the antibonding combination is empty. Each of these delocalized  $\text{Ni}_2\text{S}_2$  orbitals has  $\sim 50\%$   $\text{S}-\text{S}$  antibonding character; thus, occupation of one with an electron pair while leaving the second orbital empty can be straightforwardly extrapolated back to an overall  $\text{S}-\text{S}$  bond order of  $\sim 1/2$ , in complete agreement with an  $\text{S}:\text{S} 2c/3e$   $\sigma$  bond.<sup>35</sup>

Notably, neither of these  $\text{Ni}_2\text{S}_2$  orbitals with  $\text{S}-\text{S} \sigma^*$  character is the HOMO or LUMO of the molecule. Thus, even though

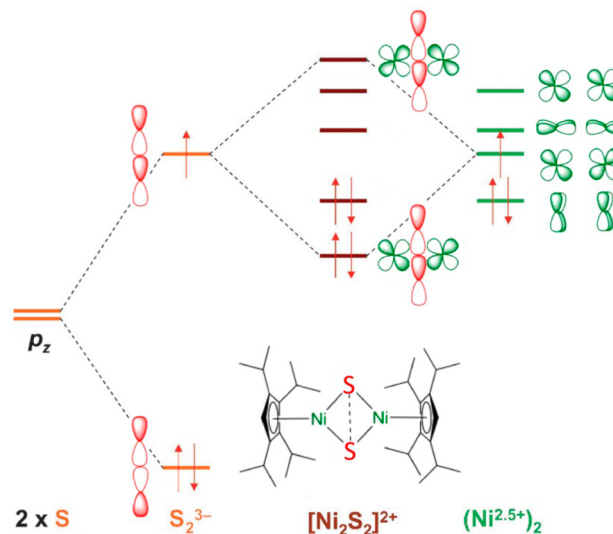


**Figure 7.** Partial molecular orbital diagram for  $\text{Cp}'_2\text{Ni}_2\text{S}_2$  highlighting the covalent interaction of the  $\text{S}-\text{S} \sigma^*$  orbital with Ni orbitals. Further interactions of the  $\text{Ni}_2$  orbitals with  $\text{S}_2$  and  $\text{Cp}' \pi$  orbitals are not shown.

one-electron reduction of  $\text{Cp}'_2\text{Ni}_2\text{S}_2$  yields an isostructural monoanion,  $[\text{Cp}'_2\text{Ni}_2\text{S}_2]^-$ , the additional unpaired electron is not considered to have " $\text{S}_2^{3-}$  radical" character. Instead, reduction of  $\text{Cp}'_2\text{Ni}_2\text{S}_2$  has been shown by XAS and XPS measurements to be Ni-centered, yielding a  $\text{Ni}_2(\text{II,II}): \text{S}_2^{3-}$  complex. In accordance with this formulation, the  $\text{S}-\text{S}$  distance in the monoanion,  $2.84 \text{ \AA}$ , is similar to that in the neutral compound.<sup>35</sup>

### A New Class of $\text{M}_2\text{S}_2$ Compounds

The  $\text{S}-\text{S}$  distances for  $\text{M}_2\text{S}_2$  compounds containing  $\text{S}_2^{2-}$ ,  $\text{S}_2^{3-}$ , and  $\text{S}_2^{2-}$  ligands are disparate enough that X-ray crystallography can be used to distinguish clearly between these cases. Plots of data for known  $\text{M}_2\text{S}_2$  and  $\text{M}_2\text{Se}_2$  compounds from the Cambridge Database with  $\text{M} = \text{V}$  through  $\text{Cu}$ , categorized by their  $\text{S}-\text{S}/\text{Se}-\text{Se}$  and  $\text{M}\cdots\text{M}$  distances, are shown in Figure 8.<sup>35</sup> Instead of displaying a continuous curve as might be expected for compounds having variable and mixed  $\text{Ch}_2^{n-}$  character with noninteger values of  $n$  ranging from 2 to 4, the compounds clearly group together in clusters. In the  $\text{M}_2\text{S}_2$  plot, there is a large group of sulfide ( $\text{S}^{2-}$ ) compounds with relatively short  $\text{M}\cdots\text{M}$  distances and  $\text{S}\cdots\text{S}$  separations  $> 3.2 \text{ \AA}$  and a second group of disulfide ( $\text{S}_2^{2-}$ ) compounds with longer  $\text{M}\cdots\text{M}$  distances and  $\sim 2.2 \text{ \AA}$   $\text{S}-\text{S}$  bonds. A third class of compounds is well separated from these, having  $\text{S}-\text{S}$  distances ranging from 2.5 to  $2.8 \text{ \AA}$ , which I propose are "sub sulfide" or  $\text{S}_2^{3-}$  compounds. The Se data are similar, and there are clear gaps in each case between clusters of compounds, suggesting that these designations are not just semantic but indicative of discrete classes of compounds with distinct physical and chemical properties.

The data in Figure 8 follow a clear trend across the transition series. The sulfide compounds are early transition metal complexes, while disulfide compounds are stabilized by late metals. The sub sulfide compounds are all complexes of Ni or Co. As shown in Figure 9, this trend is rationalized by considering the relative energies of the symmetry-matched metal and  $\text{S}-\text{S} \sigma^*$  orbitals. Subsulfido compounds will result when the energies of these two orbitals are close enough to interact covalently, as shown in the middle of Figure 9. This interaction is modulated across the transition series by the monotonic increase in effective nuclear charge ( $Z^*$ ) from left to right across the periodic table. Despite the continuous change in  $Z^*$ , the structural

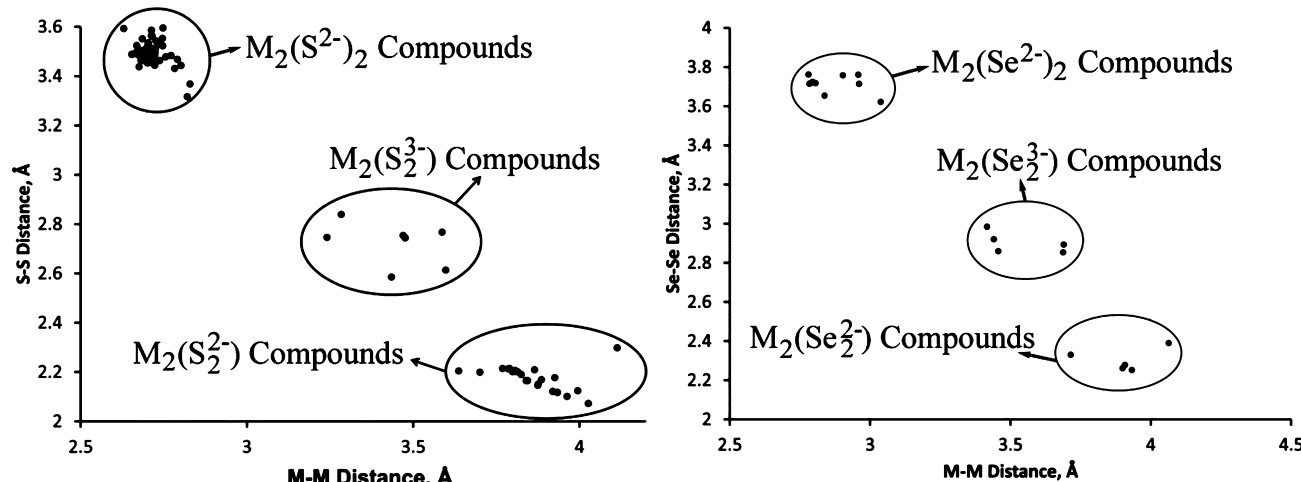


**Figure 8.** Plot of the Ch–Ch vs M···M distances in  $M_2S_2$  (right) and  $M_2Se_2$  (left) compounds from the Cambridge Database. Shown are data for the metals V through Cu. Adapted from ref 35. Copyright 2015 American Chemical Society.

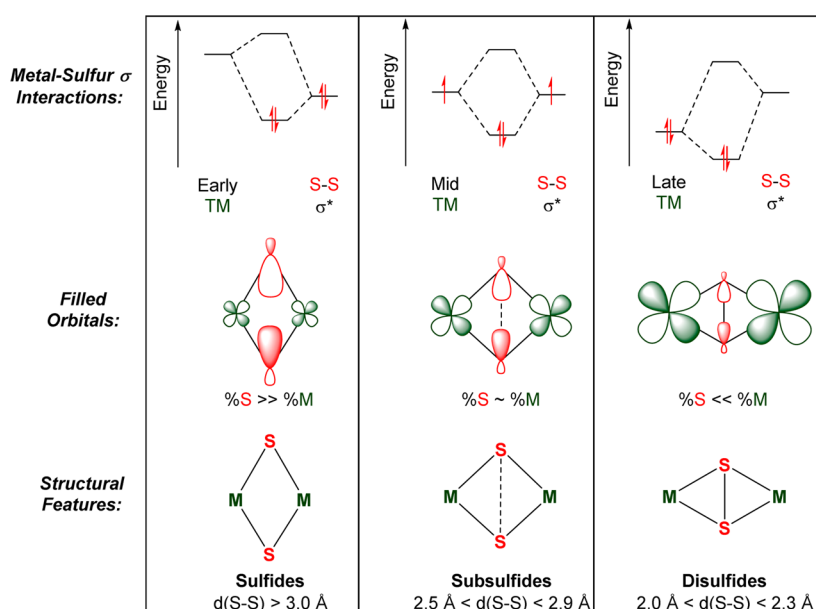


**Figure 9.** Electronic and structural properties of sulfido compounds (left), subsulfido compounds (middle), and disulfido compounds (right).

manifestations are clearly quantized. Thus, early transition metals have high-lying metal orbitals, with an electron pair originating from the S–S  $\sigma^*$  orbital of an  $S_2^{4-}$  ( $= 2 \times S^{2-}$ ) ligand. Late metals have d orbitals lower in energy than the S–S  $\sigma^*$ , leaving the latter orbital empty, as in the  $S_2^{2-}$  ligand. Subsulfido compounds thus require a delicate balance of metal and  $S_2$  orbitals, which accounts for their rarity. Undoubtedly, this theoretical framework will be of use for preparing new examples of  $Ch_2^{3-}$  compounds.

## SUMMARY

In this Account, I have traced recent history of the 2c/3e half-bond through transition metal chemistry, in  $Ni_2$ (II,III) and  $Pd_2$ (II,III) dimers, to main group chemistry, where new “subchalcogenido” ligands,  $Ch_2^{3-}$ , have been discovered. Importantly, the revelations disclosed herein have been established by judicious use of several key physical techniques and computational methods. These results highlight the power of coordination chemistry to stabilize unusual partially bonded species, which would not be stable on their own.

## AUTHOR INFORMATION

### Corresponding Author

\*E-mail: [berry@chem.wisc.edu](mailto:berry@chem.wisc.edu).

### Notes

The authors declare no competing financial interest.

### Biography

**John F. Berry** was born in Atlanta, GA, in September 1977. He attended Virginia Tech from 1996 to 2000 obtaining two degrees: a BA in composition and a BS in chemistry. John then worked as a NSF Graduate Research Fellow in the research group of F. Albert Cotton at Texas A&M University from 2000 to 2004. From 2004 to 2006, with support from the Alexander von Humboldt Foundation, he worked with Karl Wieghardt at the Max Planck Institute for Bioinorganic Chemistry in Mülheim an der Ruhr, Germany, on new routes to high-valent iron intermediates. In 2006, John joined the Department of Chemistry at the University of Wisconsin—Madison, where his group studies coordination chemistry and bonding. John still writes music in

his spare time and sometimes has occasion to perform on either the violin, viola, or piano.

## ACKNOWLEDGMENTS

I am grateful to my co-workers and collaborators, past and present, for their efforts on these projects. Funding from the National Science Foundation is gratefully acknowledged (Grants CHE-1041748 and CHE-1300464).

## REFERENCES

- (1) Pauling, L. Nature of the chemical bond. II. One-electron and three-electron bonds. *J. Am. Chem. Soc.* **1931**, *53*, 3225–3237.
- (2) Pauling, L. *The Nature of the Chemical Bond*, 3rd ed.; Cornell University Press: Ithaca, NY, 1960.
- (3) Bickelhaupt, F. M.; Diefenbach, A.; de Visser, S. P.; de Koning, L. J.; Nibbering, N. M. M. Nature of the three-electron bond in  $\text{H}_2\text{S}:\text{SH}_2^+$ . *J. Phys. Chem. A* **1998**, *102*, 9549–9553.
- (4) Maity, D. K. Sigma bonded radical cation complexes: A theoretical study. *J. Phys. Chem. A* **2002**, *106*, 5716–5721.
- (5) Li, H.; Feng, H.; Sun, W.; Zhang, Y.; Fan, Q.; Peterson, K. A.; Xie, Y.; Schaefer, H. F., III The alkaline earth dimer cations ( $\text{Be}_2^+$ ,  $\text{Mg}_2^+$ ,  $\text{Ca}_2^+$ ,  $\text{Sr}_2^+$ , and  $\text{Ba}_2^+$ ). Coupled cluster and full configuration interaction studies. *Mol. Phys.* **2013**, *111*, 2292–2298 and references therein..
- (6) Antonov, I. O.; Barker, B. J.; Bondybey, V. E.; Heaven, M. C. Spectroscopic characterization of  $\text{Be}_2^+ \text{X}^2\Sigma_u^+$  and the ionization energy of  $\text{Be}_2$ . *J. Chem. Phys.* **2010**, *133*, 074309.
- (7) Gutsev, G. L.; Bauschlicher, C. W. Chemical bonding, electron affinity, and ionization energies of the homonuclear 3d metal dimers. *J. Phys. Chem. A* **2003**, *107*, 4755–4767.
- (8) Kang, J.; Kim, J.; Ihhee, H.; Lee, Y. S. Molecular Structures, Energetics, and Electronic Properties of Neutral and Charged  $\text{Hg}_n$  Clusters ( $n = 2–8$ ). *J. Phys. Chem. A* **2010**, *114*, 5630–5639.
- (9) Drews, T.; Seppelt, K. The  $\text{Xe}_2^+$  ion - Preparation and structure. *Angew. Chem., Int. Ed. Engl.* **1997**, *36*, 273–274.
- (10) Castner, T. G.; Käenzig, W. The Electronic Structure of V-Centers. *J. Phys. Chem. Solids* **1957**, *3*, 178–195.
- (11) Cotton, F. A.; Murillo, C. A.; Walton, R. A. *Multiple Bonds between Metal Atoms*, 3rd ed.; Springer Science and Business Media, Inc.: New York, 2005.
- (12) Yam, V. W. W.; Au, V. K. M.; Leung, S. Y. L. Light-Emitting Self-Assembled Materials Based on  $d^8$  and  $d^{10}$  Transition Metal Complexes. *Chem. Rev.* **2015**, *115*, 7589–7728.
- (13) Bercaw, J. E.; Durrell, A. C.; Gray, H. B.; Green, J. C.; Hazari, N.; Labinger, J. A.; Winkler, J. R. Electronic Structures of Pd(II) Dimers. *Inorg. Chem.* **2010**, *49*, 1801–1810.
- (14) Kornecki, K. P.; Berry, J. F.; Powers, D. C.; Ritter, T. Metal-Metal Bond-Containing Complexes as Catalysts for C-H Functionalization. In *Progress in Inorganic Chemistry*, Karlin, K. D., Ed.; John Wiley & Sons: Hoboken, NJ, 2014; Vol. 58, pp 225–302.
- (15) Dahl, L. F.; Connally, N. G. Organometallic Chalcogen Complexes 20. Stereochemical Characterization of an Oxidized Iron-Sulfur Dimer,  $[\text{Fe}(\eta^5\text{-C}_5\text{H}_5)(\text{CO})(\text{SCH}_3)_2]^+$  - a Paramagnetic Cation Effectively Containing a One-Electron Metal-Metal Bond. *J. Am. Chem. Soc.* **1970**, *92*, 7472–7474.
- (16) Cotton, F. A.; Matusz, M.; Poli, R.; Feng, X. J. Dinuclear Formamidinato Complexes of Nickel and Palladium. *J. Am. Chem. Soc.* **1988**, *110*, 1144–1154.
- (17) Cotton, F. A.; Matonic, J. H.; Murillo, C. A. Completion of the series of  $\text{Pt}_2(\text{ArNC(H)NAr})_4^n$ ,  $n = 0, +1, +2$ , compounds, with Pt-Pt sigma bond orders of 0, 1/2, 1, respectively. *Inorg. Chim. Acta* **1997**, *264*, 61–65.
- (18) Berry, J. F.; Bothe, E.; Cotton, F. A.; Ibragimov, S. A.; Murillo, C. A.; Villagrán, D.; Wang, X. Metal-metal bonding in mixed valence  $\text{Ni}_2^{5+}$  complexes and spectroscopic evidence for a  $\text{Ni}_2^{6+}$  species. *Inorg. Chem.* **2006**, *45*, 4396–4406.
- (19) Yao, C. L.; He, L. P.; Korp, J. D.; Bear, J. L. Dipalladium Complexes with N,N'-Diphenylbenzamidine Bridging and Chelating Ligands – Synthesis and Structural and Electrochemical Studies. *Inorg. Chem.* **1988**, *27*, 4389–4395.
- (20) Cotton, F. A.; Gu, J. D.; Murillo, C. A.; Timmons, D. J. The first dinuclear complex of palladium(III). *J. Am. Chem. Soc.* **1998**, *120*, 13280–13281.
- (21) Berry, J. F.; Bill, E.; Bothe, E.; Cotton, F. A.; Dalal, N. S.; Ibragimov, S. A.; Kaur, N.; Liu, C. Y.; Murillo, C. A.; Nellutla, S.; North, J. M.; Villagrán, D. A fractional bond order of 1/2 in  $\text{Pd}_2^{5+}$  - Formamidinate species; The value of very high-field EPR spectra. *J. Am. Chem. Soc.* **2007**, *129*, 1393–1401.
- (22) Alvarez, S.; Hoffmann, R.; Mealli, C. A Bonding Quandary—or—A Demonstration of the Fact That Scientists Are Not Born With Logic. *Chem. - Eur. J.* **2009**, *15*, 8358–8373.
- (23) Brown, E. C.; York, J. T.; Antholine, W. E.; Ruiz, E.; Alvarez, S.; Tolman, W. B.  $\text{Cu}_3(\mu\text{-S})_2^{3+}$  clusters supported by N-donor ligands: Progress toward a synthetic model of the catalytic site of nitrous oxide reductase. *J. Am. Chem. Soc.* **2005**, *127*, 13752–13753.
- (24) Ferguson-Miller, S.; Babcock, G. T.; Yocom, C. Photosynthesis and Respiration. In *Biological Inorganic Chemistry*; Bertini, I., Gray, H. B., Stiebel, E. I., Valentine, J. S., Eds.; University Science Books: Sausalito, CA, 2007.
- (25) Armstrong, D. A.; Chipman, D. M. Structures of Sulfur-Centered Radicals. In *S-Centered Radicals*; Alfassi, Z. B., Ed.; John Wiley & Sons: Chichester, U.K., 1999.
- (26) Berry, J. F. A Definitive Answer to a Bonding Quandary? The Role of One-Electron Resonance Structures in the Bonding of a  $[\text{Cu}_3\text{S}_2]^{3+}$  Core. *Chem. - Eur. J.* **2010**, *16*, 2719–2724.
- (27) Wenska, G.; Filipiak, P.; Asmus, K.-D.; Bobrowski, K.; Koput, J.; Marciak, B. Formation of a sandwich-structure assisted, relatively long-lived sulfur-centered three-electron bonded radical anion in the reduction of a bis(1-substituted-uracyl) disulfide in aqueous solution. *J. Phys. Chem. B* **2008**, *112*, 10045–10053 and references therein.
- (28) Zhang, S.; Wang, X.; Sui, Y.; Wang, X. Odd-Electron-Bonded Sulfur Radical Cations: X-ray Structural Evidence of a Sulfur-Sulfur Three-Electron sigma-Bond. *J. Am. Chem. Soc.* **2014**, *136*, 14666–14669 and references therein.
- (29) Braida, B.; Hazebroucq, S.; Hiberty, P. C. Methyl substituent effects in  $\text{H}_n\text{X}:\text{XH}_n^+$  three-electron-bonded radical cations ( $\text{X} = \text{F}, \text{O}, \text{N}, \text{Cl}, \text{S}, \text{P}; n = 1–3$ ). An ab initio theoretical study. *J. Am. Chem. Soc.* **2002**, *124*, 2371–2378 and references therein.
- (30) Bonazzola, L.; Michaut, J. P.; Roncin, J. Radical Cations of Sulfides and Disulfides - an Electron-Spin-Resonance Study. *J. Chem. Phys.* **1985**, *83*, 2727–2732.
- (31) Sitzmann, H.; Saurenz, D.; Wolmershauser, G.; Klein, A.; Boese, R. Bis(tetraisopropylcyclopentadienylnickel)dichalcogenides: Complexes of the novel  $[\text{CpME}]_2$  type ( $\text{E} = \text{S}, \text{Se}, \text{Te}$ ). *Organometallics* **2001**, *20*, 700–705.
- (32) Yao, S.; Hrobarik, P.; Meier, F.; Rudolph, R.; Bill, E.; Irran, E.; Kaupp, M.; Driess, M. A Heterobimetallic Approach To Stabilize the Elusive Disulfur Radical Trianion ("Subsulfide")  $\text{S}_2^{3-}$ . *Chem. - Eur. J.* **2013**, *19*, 1246–1253.
- (33) Rudolph, R.; Blom, B.; Yao, S.; Meier, F.; Bill, E.; van Gastel, M.; Lindenmaier, N.; Kaupp, M.; Driess, M. Synthesis, Reactivity, and Electronic Structure of a Bioinspired Heterobimetallic  $\text{Ni}(\mu\text{-S}_2)\text{Fe}$  Complex with Disulfur Monoradical character. *Organometallics* **2014**, *33*, 3154–3162.
- (34) Sproules, S.; Wieghardt, K. Dithiolene radicals: Sulfur K-edge X-ray absorption spectroscopy and Harry's intuition. *Coord. Chem. Rev.* **2011**, *255*, 837–860.
- (35) Yao, S. A.; Martin-Diaconescu, V.; Infante, I.; Lancaster, K. M.; Goetz, A. W.; DeBeer, S.; Berry, J. F. Electronic Structure of  $\text{Ni}_2\text{E}_2$  Complexes ( $\text{E} = \text{S}, \text{Se}, \text{Te}$ ) and a Global Analysis of  $\text{M}_2\text{E}_2$  Compounds: A Case for Quantized  $\text{E}_2^{n-}$  Oxidation Levels with  $n = 2, 3$ , or 4. *J. Am. Chem. Soc.* **2015**, *137*, 4993–5011.
- (36) Yao, S. A.; Lancaster, K. M.; Goetz, A. W.; DeBeer, S.; Berry, J. F. X-ray Absorption Spectroscopic, Crystallographic, Theoretical (DFT) and Chemical Evidence for a Chalcogen-Chalcogen Two-Center/Three-Electron Half Bond in an Unprecedented "Subselenide"  $\text{Se}_2^{3-}$  Ligand. *Chem. - Eur. J.* **2012**, *18*, 9179–9183.